Thermally Curing Aryl−Ethynyl End-Capped Imide Oligomers: Study of New Aromatic End Caps

Michael E. Wright* and Derek A. Schorzman

Department of Chemistry, Virginia Commonwealth University, Richmond, Virginia 23284-2006

Laura E. Pence*

Department of Chemistry, University of Hartford, West Hartford, Connecticut 06117

Received May 24, 2000; Revised Manuscript Received September 8, 2000

ABSTRACT: Two new aryl−ethynyl end-cap model compounds, *N*-phenyl-4-(1-naphthylethynyl)phthalimide (**1**) and *N*-phenyl-4-(2-naphthylethynyl)phthalimide (**3**), were synthesized and characterized. The single-crystal molecular structure of **1** reveals an alternating "head to tail" packing mode whereas the "heads and tails" of **2** are aligned and not alternating. The thermal cure kinetics of **1** and **3** were analyzed using NMR and FT-IR spectroscopy, respectively, and compared to *N*-phenyl-4-phenylethynylphthalimide (**2**). In both cases the naphthyl−ethynyl model compounds reacted faster than the phenyl−ethynyl derivative. The end-capped imide oligomers analogues of **1** and **2**, NETI-5 and PETI-5, respectively, were synthesized and their thermal cure kinetics were analyzed by DSC. The thermal cure kinetics of **1** and **2** best fit a first-order rate law. Compound **1** cures at faster rates than **2**, although the calculated E_a values of **1** and **2** are statistically indistinguishable. The thermal cure kinetics of **2** and **3** also fit a first-order rate law and show that the E_a of **3** is higher than that of **2**, although **3** thermally cures at slightly faster rates than **2**, but slower than **1** (^{1}H NMR) at the temperatures studied. The E_a values determined for **2** by ^{1}H NMR and by FT-IR differ significantly. The DSC thermal cure kinetics of NETI-5 and PETI-5 best fit a first-order rate law and revealed a rate acceleration trend similar to that observed for the model compounds **1** and **2**. Effectively, NETI-5 cures at the same rate as PETI-5 but at approximately a 30 °C lower curing temperature.

Introduction

Phenyl−ethynyl terminated imide oligomers can be thermally cured to afford a final resin that possesses excellent mechanical and chemical properties pivotal to high-performance composite applications.[1−17] The cured phenyl−ethynyl terminated resins possess improved therm-oxidative stability and processability over thermally cured acetylene-terminated imide oligomer resins.[14,18] Typical curing temperatures for the neat oligomer are generally near 350 °C and the chemical reaction(s) leading to the final resin appear to be multifaceted. It has been suggested that curing may be through a free-radical cross-linking and/or extension reaction(s). A variety of possible cured resin structures have been proposed, primarily from reaction(s) of the acetylene bond.[1a] The entire cure process appears to follow a complicated rate law.[1b,11] Some of the most recent studies have suggested that first-order (*pseudo*) kinetics are followed for the initial 90% of the reaction for both an oligomeric material and a bis(phenyl−ethynyl) model compound.[1b] Other mechanistic studies have demonstrated the complexity of the curing process.[11] It is interesting to note that, in each study performed to date, there is reasonably good agreement between the kinetic data observed for oligomeric material and their model compound analogues. This latter point would appear to validate the use and study of small molecules to probe both the mechanism and products for at least a majority of the curing reaction(s).We recognized from a review of the literature that no previous studies had explored the incorporation of polycyclic aromatic rings in aryl−ethynyl end-capping groups. This substitution would appear to provide the necessary thermal stability and provide a significant change in stereoelectronics. Our research interests include the kinetic analysis of the thermal curing of several aryl−ethynyl phthalimide model compounds and corresponding oligomers in an attempt to elucidate the thermal curing reaction(s) and to develop faster curing materials while retaining the desirable properties of NASA's thermally cured PETI-5 (phenyl−ethynyl terminated imide) oligomer.[2]

Chart 1

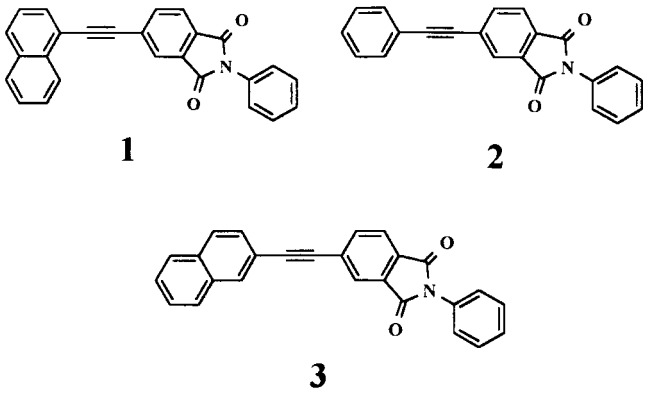

Results and Discussion

Model Compounds and Imide Oligomer Syntheses. Model compounds *N*-phenyl-4-(1-naphthylethynyl)-phthalimide (**1**), *N*-phenyl-4-phenylethynylphthalimide (**2**), and *N*-phenyl-4-(2-naphthylethynyl)phthalimide (**3**) were prepared in good yield using standard ethynylation techniques (Chart 1).[19] It was interesting to find that

10.1021/ma000916q CCC: $19.00
Published on Web 10/14/2000

Table 1. Arrhenius Analysis of Kinetic Data for Model Compounds and Oligomers

analysis method	^{1}H NMR	^{1}H NMR	FTIR	FTIR	DSC	DSC
sample	**1**	**2**	**2**	**3**	PETI-5	NETI-5
R^2	0.9969	0.9986	0.9989	0.9998	0.9997	0.9968
slope[a]	−22639 (897)	−21411 (464)	−15172 (494)	−23877 (349)	−18810 (347)	−19556 (1111)
intercept[a]	35.23 (157)	31.49 (80)	20.75 (85)	36.75 (60)	25.09 (56)	27.46 (178)
E_a (kcal/mol)[a]	44.99 (178)	42.55 (92)	30.15 (98)	47.45 (69)	37.38 (69)	38.86 (221)
A (min^{-1})	10^{15}	10^{13}	10^{9}	10^{15}	10^{10}	10^{11}

[a] Number in parentheses represents the standard deviation error for the last significant digits.

Table 2. Eyring Analysis of Kinetic Data for Model Compounds and Oligomers

analysis method	^{1}H NMR	^{1}H NMR	FTIR	FTIR	DSC	DSC
sample	**1**	**2**	**2**	**3**	PETI-5	NETI-5
R^2	0.9967	0.9985	0.9988	0.9998	0.9996	0.9996
slope[a]	−22067 (899)	−20830 (466)	−14590 (500)	−23295 (355)	−18187 (341)	−18933 (1116)
intercept[a]	27.88 (157)	24.13 (80)	13.38 (86)	29.38 (61)	17.65 (55)	20.03 (179)
ΔH_{act}[a] (kcal/mol)	43.85 (179)	41.39 (93)	28.99 (99)	46.29 (71)	36.14 (68)	37.62 (222)
ΔS_{act}[a] (cal/K mol)[a]	8.1 (31)	0.6 (16)	−20.7 (17)	11.1 (12)	−12.2 (11)	−7.5 (36)

[a] Numbers in parentheses represent standard deviation error for the last significant digits.

Table 3. Observed Rates of Thermal Cure for Model Compounds and Oligomers at All Temperatures Studied

analysis method	sample	270 °C	290 °C	310 °C	330 °C	350 °C	370 °C
^{1}H NMR	**1**	1.57×10^{-3}	6.53×10^{-3}	3.18×10^{-2}	9.26×10^{-2}		
^{1}H NMR	**2**	3.53×10^{-4}	1.43×10^{-3}	6.09×10^{-3}	1.68×10^{-2}	5.71×10^{-2}	
FTIR	**2**		2.01×10^{-3}	5.33×10^{-3}	1.20×10^{-2}		
FTIR	**3**		3.48×10^{-3}	1.55×10^{-2}	5.79×10^{-2}		
DSC	NETI-5				6.78×10^{-3}	2.12×10^{-2}	5.09×10^{-2}
DSC	PETI-5				2.27×10^{-3}	5.9×10^{-3}	1.58×10^{-2}

Scheme 1

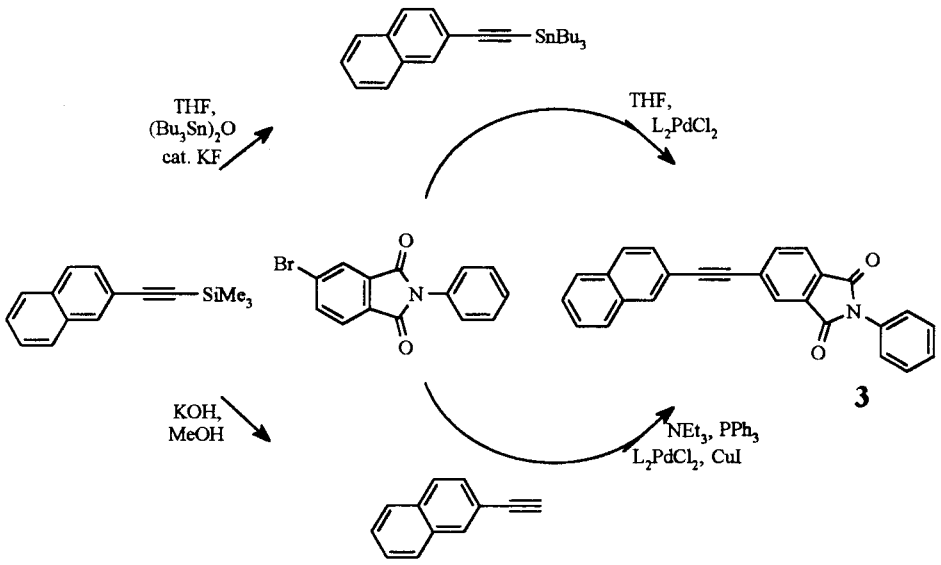

compound **3** exhibited a unique lack of solubility in chloroform. This combined with spectral peak overlaps initially made us doubtful if indeed we had the correct compound in hand. Thus, we synthesized **3** using two independent synthetic pathways (Scheme 1). In each case, the same identical product was produced and has been unambiguously assigned the structure of **3** based on spectroscopic and analytical data.

The PETI-5 (phenyl−ethynyl terminated imide oligomer) and NETI-5 (naphthyl−ethynyl terminated imide oligomer) oligomers were prepared to a theoretical molecular weight of 5000 using the previously reported technique.[7] The NETI-5 oligomer incorporated our new end-capping reagent, 4-(1-naphthylethynyl)phthalic anhydride (4-NEPA). As expected, the naphthyl moiety showed no discernible effect on the reactivity of the anhydride group, and the oligomeric materials were generated in very good yield. NETI-5 displayed similar physical properties (e.g., T_g) and solubility in common organic solvents.

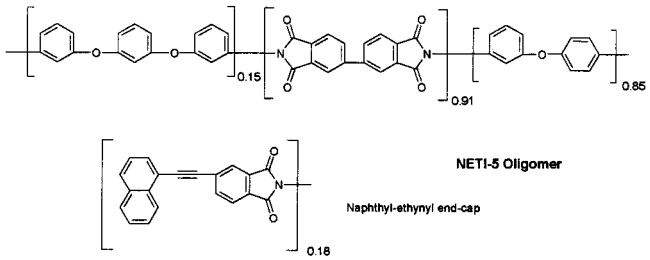

To better understand the reactivity differences we find in the aryl−ethynyl moieties, a series of single-crystal molecular structure determinations on the model compounds have been carried out. Single crystals of **1** and **2** were obtained by diffusing pentane into a

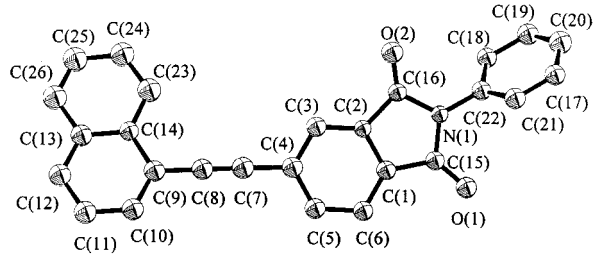

Figure 1. ORTEP view of *N*-phenyl-4-(1-naphthylethynyl)-phthalimide, molecule **1a**, showing the 50% probability thermal ellipsoids. The hydrogen atoms are omitted for clarity.

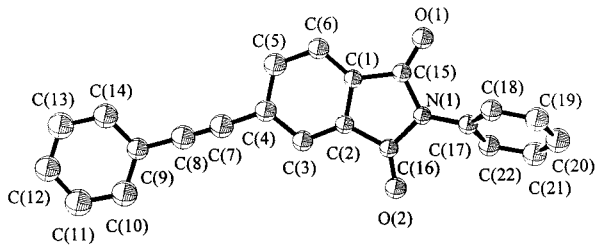

Figure 2. ORTEP view of *N*-phenyl-4-phenylethynylphthalimide (**2**) showing the 50% probability thermal ellipsoids. The hydrogen atoms are omitted for clarity.

chloroform solution containing the appropriate compound. Drawings for the molecular structures are displayed in Figures 1 and 2. Complete details (atomic coordinates, bond angles and lengths, etc.) for the structure determinations can be found in the Supporting Information.

Overall, we find that the bond distances for structures of **1** and **2** show no significant differences in key functional group areas. For example, the alkyne linkage in **1** we observe bond distances for C(4)−C(7), C(7)−C(8), and C(8)−C(9) of 1.46 (1), 1.19 (1), and 1.41(1) Å, respectively. A comparison to **2** reveals bond distances of 1.41(1), 1.21(1), and 1.42(1) Å. The presence of three molecules in the asymmetric unit of the 1-naphthyl−ethynyl structure **1** offers an unusual opportunity to compare three examples of the same structure under the same conditions. The structure consists of three rigid ring systems linked through two points of flexibility or twist. The phenyl rings bonded to the N of the phthalimide have similar torsion angles of 124, 126, and 127° in the three molecules respectively, typical for systems with no ortho substituents on the phenyls.[20−22] The ethynyl triple bond represents the second source of twist in the molecules. Two of the molecules, molecule **1a** and molecule **1b** (as shown in Figure 1), have a torsion angle of 160 and 162°, respectively, between the phthalimide ring system and the naphthyl ring system. In molecule **1c**, the angle is only 8° for the same measurement resulting in an orientation in which the bulk of the naphthyl ring is on the same side as C(5) and C(6) of the phthalimide moiety in comparison to molecules **1a** and **1b** in which the bulk of the naphthyl ring is on the opposite side from atoms C(5) and C(6).

We find that the molecular packing for the two molecular structures shows a very intriguing difference (Figures 3 and 4). The asymmetric unit as shown in Figure 3 demonstrates the similarity between the outer molecules **1a** and **1b**, but the lack of an inversion center is clearly displayed by the presence of molecule **1c** in the center, which confirms the choice of the acentric space group. The phenyl−ethynyl structure, **2**, crystallizes with a single molecule in the asymmetric unit.

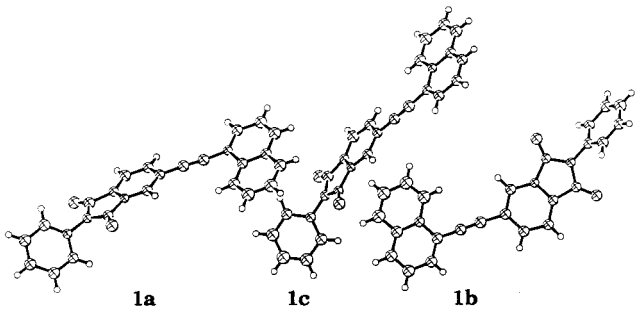

Figure 3. ORTEP view of the asymmetric unit for compound **1** displaying molecule **1c** in the center between molecules **1a** and **1b**.

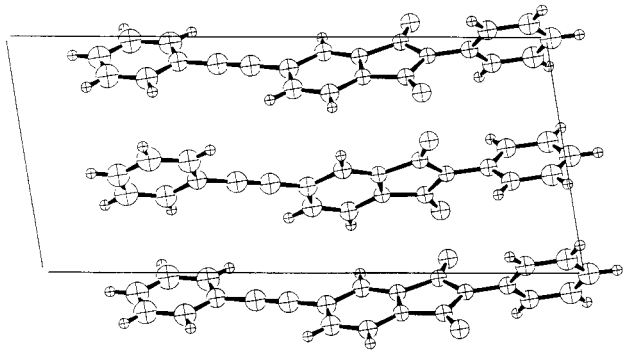

Figure 4. Unit cell packing diagram of **2** looking down the *b* axis. The rear layer, which has an orientation identical to the front layer shown, has been omitted for clarity.

Examination of the packing diagram in Figure 4 shows that the molecules pack with "heads and tails" aligned and not alternating, again removing the inversion center and verifying the low symmetry space group. This packing mode contrasts with asymmetric unit of **1** in which the molecules instead orient head to tail, and as a result do not display the complementary conformations shown in Figure 4. The extremely efficient packing of **2** (d_{calcd} = 1.343 g cm^{-3}) is demonstrated by close intermolecular contacts under 3.0 Å for O(1)−C(16), O(1)−O(2), O(1)−N(1), O(2)−C(15), and O(2)−N(1), although the lack of ring stacking is indicated by only two unimportant C−C contacts under 3.6 Å, 3.52(1) Å for C(3)−C(6) and 3.56(2) Å for C(11)−C(14). Overall compound **1** packs more densely (d_{calcd} = 1.352 g cm^{-3}) even though the closest intermolecular contacts are approximately 3.2 Å each from O(2)−C(16), O(102)−C(116), and O(201)−C(110). At this time it is unclear how these differences in packing directly relate to the difference in reactivity (i.e. rate of curing) for compounds **1** and **2**. However, the crystal structures do show that when the molecules approach in the condensed state there are distinct differences found in the intermolecular arrangements and forces.

Acquiring Kinetic Data for the Curing Reactions. For each of the model systems studied, an array of sealed glass tubes each containing a known amount of model compound was heated. At specified reaction times a single glass tube was removed from the heating block and cooled to ambient temperature. The remaining samples in the heating block were unaffected by each sample removal.

The excellent $CDCl_3$ solubility of **1** and **2**, both before and after thermal cure, permitted us to employ proton NMR spectroscopic analysis as to measure the kinetics of curing. More specifically, the aromatic protons of **1**

and **2** are found to move upfield and collapse into a single broad peak (approximately δ 7−8 ppm) as the thermal curing process moves along. Each sample was completely dissolved in $CDCl_3$ that contained an integration standard of 1,2-dichloroethane. The concentration of unreacted model compound was determined directly by integration of the proton NMR signals for the phthalimide singlet (**1**, δ 8.20; **2**, δ 8.08) to the 1,2-dichloroethane singlet (δ 3.73 ppm). In addition, we observed an induction period (time $\propto$ temperature^{-1}) for each sample that we attribute to equilibration to the heating block temperature. Applying first-order data analysis (ie. $\ln(C/C_0)$ vs time), we obtained uniformly good line fits and used the observed rate constants (k) in Arrhenius plots to determine the energy of activation (E_a) and Eyring plots (i.e. $\ln[(C/C_0)/T]$ vs $1/T$) to determine thermodynamic parameters. To strike a better comparison we also performed ^{1}H NMR kinetic analysis on the phenyl−ethynyl model compound (**2**). Several samples were analyzed by size exclusion chromatography (SEC) by dilution in THF (2 mg/mL) and then injection onto a Hewlett-Packard 1100 HPLC (column: PL 300 × 7.5 mm, 5 μm particle size). Molecular weights are calculated relative to polystyrene standards.

Poor solubility of **3** in $CDCl_3$ precluded us from performing a ^{1}H NMR spectro-kinetic analysis. As before, compounds **2** and **3** were thermally cured, but now each sample was mixed with KBr and formed into a pellet and then analyzed on a Nicolet Magna FT-IR 760 spectrometer. Concentrations for the reactant model compound were determined by integration of the alkyne $\nu_{C\equiv C}$ stretch (**2**, 2216 cm^{-1}; **3**, 2209 cm^{-1}) to the integration of the ν_{C-H} peaks (**2**, 3068−3018 cm^{-1}; **3**, 3058−3032 cm^{-1}). The ν_{C-H} peaks offered an ideal internal integration standard due to the occurrence in a region free from other peaks and with an intensity similar to that of the alkyne $\nu_{C\equiv C}$ peak. In addition, no gaseous byproducts were detected during the thermal cure of the model compounds, as has been previously reported for PETI-5 and other model compounds.[3] The induction period consisted of an increase in alkyne stretch intensity relative to the internal standard peak(s) to approximately 130% of the initial value. We attribute this increase in intensity to a reorganization of the molecules within the solid state. Applying first-order analysis for data following the induction period, we obtained uniformly good line fits and used these rate constants in Arrhenius and Eyring plots. The analyses were also performed on the phenyl−ethynyl model compound (**2**) as our reference point.

The kinetic analysis of the oligomeric systems of PETI-5 and NETI-5 were also carried out as above; however, due to a lack of solubility and dilution of the ethynyl functional group the progress of the reaction was followed by DSC. Hence, at various time intervals, a sample was removed from the heating block and then analyzed on a Perkin-Elmer DSC-7 (under dinitrogen, flow rate of 40 cm^3/min, ramp rate of 10 °C/min). The extent of cure was calculated using the DiBenedetto equation, modified for highly cross-linked networks:[1b,23−26]

$$(T_g - T_{gu})/(T_{gc} - T_{gu}) = \lambda x/(1 - (1 - \lambda)x)$$

where T_g represents the glass transition temperature of the model compound after thermal curing at each temperature, T_{gu} is the glass transition temperature of the uncured model compound, T_{gc} is the glass transition temperature of fully cured model compound, λ is the ratio of the isobaric heat capacity of fully cured model compound to that of uncured model compound, and x is the reaction extent (i.e. $C/C_0 = 1 - x$). DSC analysis of uncured NETI-5 revealed a melting peak at 264 °C in the first scan and a T_{gu} of 230 °C in the second scan. Similarly, uncured PETI-5 consisted of a melting peak at 263 °C in the first scan and a T_{gu} of 237 °C in the second scan. The λ and T_{gc} values determined by Fang et al.[1b] corresponded well with both NETI-5 and PETI-5 and were used in our calculations ($\lambda = 0.69$, $T_{gc} = 69.9$ °C). It has been previously reported that properties of the imide oligomers and the cured resins are nearly identical regardless of the end-capping compound. Applying first-order data analysis, we obtained uniformly good line fits and used the observed rate constants in Arrhenius and Eyring plots.

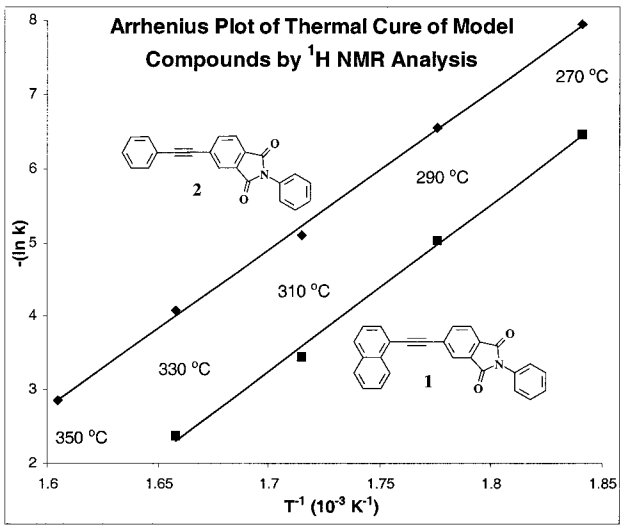

Figure 5. Arrhenius plot of thermal cure kinetics of model compounds **1** (■) and **2** (◆). Regression data and calculated Arrhenius parameters are provided in Table 1.

Analyses of the Kinetic Data for the Thermal Curing Reaction. Analysis of the thermal cure of model compounds **1** and **2** by ^{1}H NMR spectroscopy followed by Arrhenius parameter evaluation revealed statistically indistinguishable energies of activation (E_a) (Figures 5 and 6). However, the 1-naphthyl−ethynyl model compound (**1**) was found to cure significantly faster then the phenyl−ethynyl model compound (**2**) at any temperature studied. The difference in rates can be attributed to the preexponential factor (A), which accounts for stereoelectronic effects, collisional parameters, etc. Unfortunately, the interpretation of A is difficult, and the extrapolation error is large. In terms of the thermodynamic parameters determined by Eyring analysis of the kinetic data, the difference in rates can be attributed to different activation entropies (ΔS_{act}) of **1** and **2**, whereas the activation enthalpies (ΔH_{act}) are statistically indistinguishable. SEC analyses of several of the cured samples were found to correlate well with the calculated C/C_0 values (Figure 7). The nearly identical SEC traces of **1** and **2** are consistent with the formation of trimeric product with no higher molecular weight products detected even near the completion of the curing process (i.e. $C/C_0 = 0$). FT-IR analysis of the thermal cure kinetics of model compounds **2** and **3** via loss of the alkyne stretch peak revealed that the 2-naphthyl−ethynyl model (**3**) has a significantly higher $E_a/\Delta H_{act}$ than the phenyl−ethynyl model (**2**). **3** under-

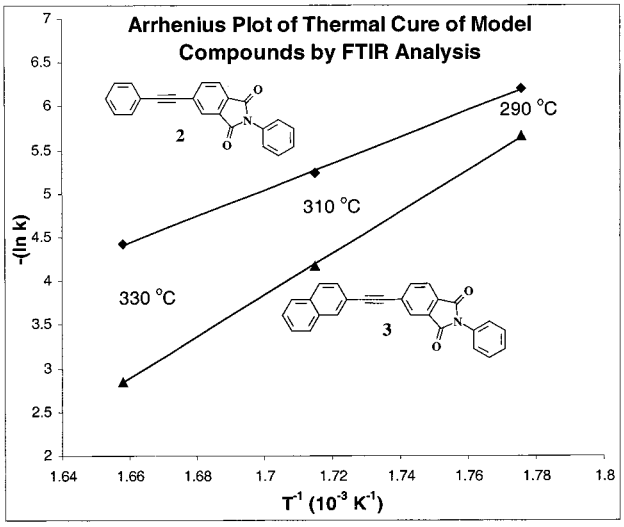

Figure 6. Arrhenius plot of thermal cure kinetics of model compounds **2** (◆) and **3** (▲). Regression data and calculated Arrhenius parameters are provided in Table 1.

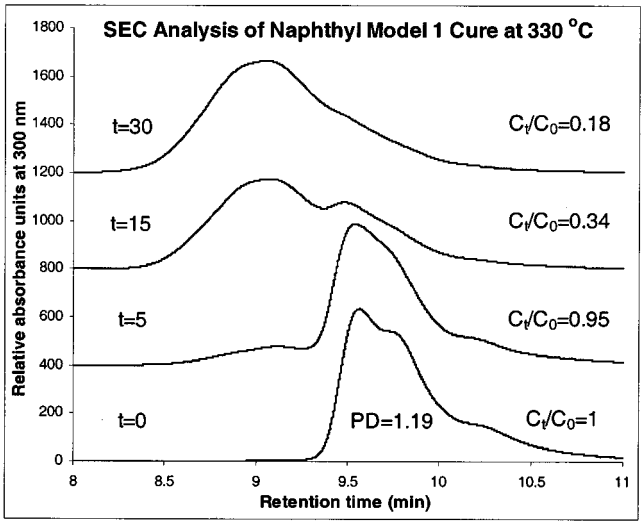

Figure 7. SEC traces of cured model compound **1** at 330 °C. Reaction time, reaction extent (C_t/C_0), and polydispersity (PD) of uncured **1** are indicated.

goes thermal curing at faster rates than **2**, but slower than **1** at the temperatures studied. In addition, the $E_a/\Delta H_{act}$ of **2** as determined by FT-IR analysis is significantly lower than determined by ^{1}H NMR analysis. Insolubility of **3** in common organic solvents prevented SEC analysis.

DSC analysis (Figure 8) of PETI-5 and NETI-5 revealed a trend similar to that found in model compounds **1** and **2**. The $E_a/\Delta H_{act}$ values of the oligomers were statistically indistinguishable, but the thermal cure rate of NETI-5 was found to be approximately three times faster than PETI-5 at all temperatures studied (Figure 9). Thus, NETI-5 can be cured at the same rate as PETI-5 but at approximately a 30 °C lower cure temperature. It is important to mention that in the literature cure rates for PETI-5 appear faster than measured and reported in our study. We believe this shows the importance of testing a standard, like PETI-5, to "calibrate" the reactivity of the new end-capping group. The very slight reduction in rate acceleration for the oligomer when compared to the model compound may be due to lower concentration of end caps in the oligomers when compared to neat in **1** and **2** and/or the

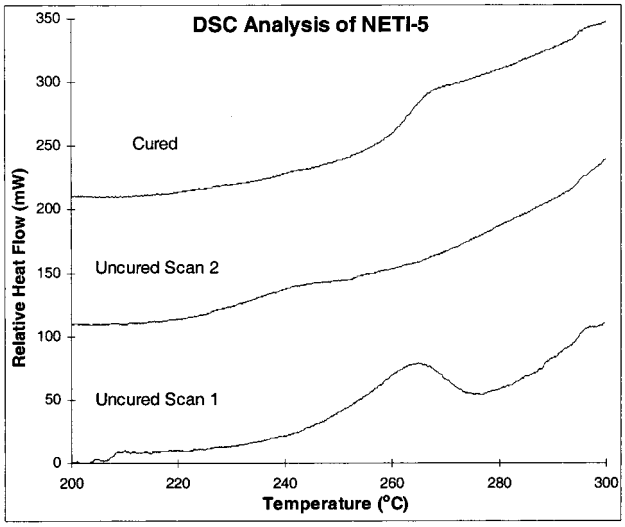

Figure 8. DSC traces of first and second scans of uncured NETI-5 and cured NETI-5 (1 h at 380 °C).

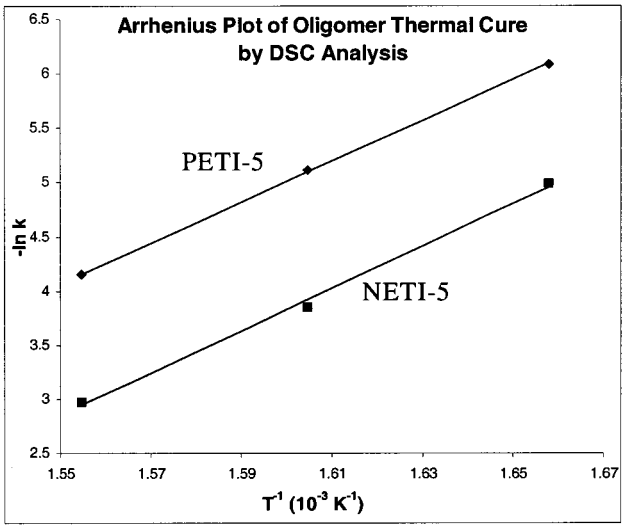

Figure 9. Arrhenius plot of thermal cure kinetics of NETI-5 (■) and PETI-5 (◆). Regression data and calculated Arrhenius parameters are provided in Table 1.

reduced mobility of the reactive group on the fairly rigid imide backbone. Nevertheless, it is gratifying to see the model compounds accelerated curing reaction do translate to the oligomeric system very well.

Concluding Remarks

In this study, we demonstrate by ^{1}H NMR spectroscopy that the 1-naphthyl−ethynyl imide model compound **1** cures significantly faster than the phenyl analogue. In addition the 2-naphthyl−ethynyl imide (**3**) model compound also cures faster than the phenyl, but not as fast as compound **1**. The rate acceleration of the 1-naphthyl−ethynyl model permits a similar cure rate but at a temperature nearly 30 °C lower. At this point in time it appears by ^{1}H NMR spectroscopy and SEC analysis that the thermal curing reaction(s) of **1**−**3** lead to similar products (possibly trimers). Interestingly, the single-crystal molecular-structures for **1** and **2** show a distinct difference in packing arrangements. It could be this difference in intermolecular packing (i.e., attractions) that may account for the significant differences in curing rates we have measured for the different aryl−ethynyl compounds. It is also important to mention that

the reaction rates measured for the thermal cure of **2** by two methods of spectroscopic analysis (^{1}H NMR and FTIR spectroscopy) afford significantly different, as are the calculated Arrhenius and Eyring parameters. Hinckley has also reported a similar lack of one-to-one correlation. These data show the importance of utilizing a reference compound, like **2**, to help standardize new compounds and new ways of measuring cure processes.

A key aspect to this work was the demonstration that the rate acceleration observed in the thermal cure of the model compound is also observed in the double end-capped imide oligomers. The net result is that we have developed naphthyl−ethynyl terminated imide (NETI-5) oligomer which will cure at competitive rates; however, at a significantly lower temperature (∼30 °C). Work is continuing in our laboratories to understand the reaction rate enhancements and to use this knowledge to design and tailor the curing process of other new aryl−ethynyl end-capped imide oligomers and polymers.

Experimental Section

General Methods. All manipulations of compounds and solvents were carried out using standard Schlenk techniques. Tetrahydrofuran (THF) and triethylamine were purified by distillation under nitrogen from standard drying agents. *N*-Methylpyrrolidinone was dried over molecular sieves prior to use. ^{1}H and ^{13}C NMR measurements were performed using a Varian Oxford 300 MHz instrument. NMR chemical shifts are reported versus Me_4Si in ^{1}H NMR spectra and assigning the $CDCl_3$ resonance at 77.00 ppm in ^{13}C NMR spectra. The compounds 1-bromonaphthalene, 2-bromonaphthalene, 3,4′-oxydianiline, and 3,3′,4,4′-biphenyltetracarboxylic anhydride were purchased from Aldrich Chemical Co. The compound 1,3-bis(3-aminophenoxy)benzene was purchased from TCI America and trimethylsilylacetylene was purchased from GFS Chemicals, Inc. 4-Bromophthalic anhydride was supplied by NASA, Langley, VA. SEC analyses were performed by dilution in THF (2 mg/mL) and then injection onto a Hewlett-Packard 1100 HPLC (column: PL 300 × 7.5 mm, 5 μm particle size). Molecular weights are calculated relative to polystyrene standards. Elemental analyses were performed at Atlantic Microlab Inc., Norcross, GA.

Synthesis of (*N*-Phenyl)-4-(1-naphthylethynyl)phthalimide. A flask charged with a 1:1 benzene/triethylamine mixture (30 mL), 4-(*N*-phenyl)-bromophthalimide (906 mg, 3.0 mmol), cuprous iodide (0.15 mmol, 30 mg), bis(triphenylphosphine)palladium dichloride (0.06 mmol, 40 mg), and triphenylphosphine (0.30 mmol, 80 mg) was treated with 1-naphthylacetylene (3.90 mmol, 600 mg) and heated at reflux for 3 h. The mixture was then cooled and filtered. The solid product was stirred in water (100 mL), filtered, and washed with water (3 × 10 mL). The crude product was recrystallized from toluene and vacuum-dried at 85 °C to yield a yellow solid (560 mg, 50.0%): mp 176−178 °C; ^{1}H NMR ($CDCl_3$, 300 MHz) δ 7.40−7.68 (m, 8 H), 7.83 (d, J = 7.2 Hz, 1 H), 7.91 (dd, J = 6.5, 4.7 Hz, 1 H), 7.98 (d, J = 7.8 Hz, 1 H), 8.03 (d, J = 7.5 Hz, 1 H), 8.20 (s, 1 H), 8.42 (d, J = 8.4 Hz, 1 H); ^{13}C NMR ($CDCl_3$, 300 MHz) δ 92.7, 92.9, 119.8, 124.0, 125.5, 126.1, 126.69, 126.72, 126.9, 127.4, 128.4, 128.7, 129.4, 130.1, 130.2, 130.5, 131.3, 131.8, 132.2, 133.32, 133.35, 137.3, 166.8. Anal. Calcd for $C_{26}H_{15}NO_2$: C, 83.63; H, 4.05. Found: C, 83.67; H, 4.12.

Synthesis of 4-(1-Naphthylethynyl)phthalic anhydride (4-NEPA). To a solution of 4-bromophthalic anhydride (4.54 g, 20.0 mmol), triphenylphosphine (520 mg, 2.0 mmol), cuprous iodide (190 mg, 1.0 mmol), and bis(triphenylphosphine)-palladium dichloride (280 mg, 0.4 mmol) in 2:1 triethylamine/benzene (75 mL) was added 1-ethynylnaphthalene (4.94 g, 32.5 mmol) in benzene (25 mL) by cannula transfer, and the mixture was heated at reflux for 2 h. The cooled solution was filtered, and the precipitate was added to water (150 mL), filtered, and washed with water (3 × 5 mL). The crude yellow solid was recrystallized from toluene, filtered, and washed with hexanes (3 × 5 mL). The product was then added to 0.15 M $NaHCO_3$(aq), stirred vigorously for 1 h, and filtered. The yellow solid was dried at reduced pressure to constant weight to yield 4-(1-naphthylethynyl)phthalic anhydride (2.16 g, 36.2%). mp 220−222 °C; ^{1}H NMR ($CDCl_3$, 300 MHz) δ 7.48−7.68 (m, 3 H), 7.82 (d, J = 7.2 Hz, 1 H), δ 7.92 (t, J = 8.1 Hz, 2 H), δ 7.99 (d, J = 7.8 Hz, 1 H), δ 8.07 (d, J = 8.0 Hz, 1 H), δ 8.20 (s, 1 H), δ 8.35 (d, J = 8.1 Hz, 1 H); ^{13}C NMR ($CDCl_3$, 300 MHz) δ 92.0, 94.6, 119.3, 125.5, 125.8, 125.9, 127.0, 127.6, 128.4, 128.8, 129.7, 130.6, 131.7, 131.9, 132.2, 133.3, 133.4, 138.7, 162.3, 162.3. Anal. Calcd for $C_{20}H_{10}O_3$: C, 80.53; H, 3.38. Found: C, 80.37; H, 3.36.

General X-ray Crystallographic Procedures. Crystalline samples of **1** and **2** were inspected by microscopy and were examined a CAD4 diffractometer equipped with graphite-monochromated Mo Kα radiation (λ = 0.710 73 Å). Details of the data collection and refinement are included in Table E (Supporting Information).

X-ray Structure Determination for *N*-Phenyl-4-(1-naphthylethynyl)phthalimide (1). An irregular shaped yellow specimen of approximate dimensions 0.41 × 0.38 × 0.20 was cut from a larger block and was mounted with Infinium Parabar 10312 oil at low temperature on a quartz fiber. The crystal was judged to be of acceptable quality by the collection of several ω scans whose average width at half-height was 0.288°. The orthorhombic symmetry was confirmed by axial photography. Three periodically monitored intensity check reflections displayed no decay of intensity throughout data collection. An empirical absorption correction was applied to the data. The data were actually collected for monoclinic symmetry, but the redundant data were averaged prior to final refinement. The structure was solved by using the teXsan software package.[27] Although attempts to solve in the centric space group, *Pbcm* (57) were unsuccessful and SHELX 97 produced poor FOM's, all of the non-hydrogen atoms of the three molecules in the asymmetric unit were revealed by the application of SHELX 97[28] in the acentric space group, $Pca2_1$ (29). The rapid falloff of diffraction intensity at high angle coupled with the need to refine three molecules in the unit cell produced an unfortunately small data-to-parameter ratio of 5.4:1**,** despite refining the non-hydrogen atoms isotropically rather than anisotropically. Hydrogen atoms were included in calculated positions. The twist of each of the molecules and lack of any correlation coefficients greater than 0.5 in the final least squares cycle was further evidence that acentric space group was the correct choice. The maximum residual electron density was 0.27 $e^-/Å^3$ in the final difference map.

X-ray Structure Determination for *N*-Phenyl-4-phenylethynylphthalimide (2). A colorless triangular plate measuring approximately 0.28 × 0.30 × 0.33 mm was mounted with epoxy on the end of a quartz fiber. The quality of the crystal was established by five ω scans whose average widths at half-height were less than 0.300°, and the monoclinic symmetry was confirmed by axial photographs. Three periodically monitored intensity check reflections indicated a decay of only 0.5% throughout the course of data collection so a decay correction was not applied to the data. As with the previous structure, there was some difficulty establishing the correct space group. Attempts to solve the data in $P2/a$ (no. 13, cell choice no. 3) or $P2_1/a$ (no. 14) produced only the phthalimide moiety plus an incomplete phenyl ring off the nitrogen with R factors above 0.3. Application of the SHELX 97 solution program in the space group, *Pa* (no. 7, cell choice no. 3), revealed all of the non-hydrogen atoms in the structure with R factors under 0.1 even for the first least-squares refinement. Analysis of the packing diagram verified the acentric symmetry of the unit cell (vide supra). All non-hydrogen atoms were refined isotropically; Hydrogen atoms were included in calculated positions. The final difference map displayed a maximum residual electron density of 0.28 $e^-/Å^3$.

Synthesis of Naphthyl−Ethynyl Terminated Imide Oligomer (NETI-5). To a solution of 1,3-bis(3-aminophenoxy)-benzene (0.15 equiv, 0.19 g, 0.66 mmol) and 3,4′-oxydianiline (0.85 equiv, 0.75 g, 3.8 mmol) in *N*-methylpyrrolidinone (35 mL) at 0 °C were added 3,3′,4,4′-biphenyltetracarboxylic

dianhydride (0.91 equiv, 1.18 g, 4.02 mmol) and 4-(1-naphthylethynyl)phthalic anhydride (0.18 equiv, 0.24 g, 0.79 mmol). The solution was warmed to 25 °C and stirred under a nitrogen atmosphere for 20 h. The flask was equipped with a Dean−Stark trap and condenser, toluene was added (100 mL), and the mixture was heated at reflux for approximately 20 h. The cooled solution was filtered and the precipitate added to water (150 mL), filtered, and washed successively with warm water (3 × 10 mL) and methanol (3 × 10 mL). The powders were then dried at 85 °C and reduced pressure to constant weight to yield NETI-5 (2.82 g, 96.6%): $M_w = 2907$; PD = 1.66.

Acknowledgment. M.E.W. is grateful to VCU for funding this research and NASA for supplying us the 3-bromophthalic anhydride. We would also like to thank Prof. Sally Hunnicutt and Dr. Bev Vincent for partaking in several helpful discussions.

Supporting Information Available: Complete listings of atomic coordinates, isotropic thermal parameters, bond distances and angles, and details of data collection. This material is available free of charge via the Internet at http://pubs.acs.org.

References and Notes

(1) (a) Fang, X.; Xie, X.-Q.; Simone, C. D.; Stevens, M. P.; Scola, D. A. *Macromolecules* **2000**, *33*, 1671 and references therein. (b) Fang, X.; Rogers, D. F.; Scola, D. A.; Stevens, M. P. *J. Polym. Sci.* **1998**, *36*, 461−470.
(2) Wright, M. E.; Schorzman, D. A. *Macromolecules* **1999**, *32*, 8693−8694.
(3) Connell, J. W.; Smith, J. G., Jr.; Hergenrother, P. M. *High Perform. Polym.* **1998**, *10*, 273−283. For related phenyl−ethynyl curing materials, see: Douglas, W. E.; Overend, A. S. *Eur. Polym. J.* **1993**, *29*, 1513.
(4) Jayaraman, S.; Srinivasan, R.; McGrath, J. E. *J. Polym. Sci., Part A* **1995**, *33*, 1551−1563.
(5) Hergenrother, P. M.; Bryant, R. G.; Jensen, B. J.; Haves, S. J. *J. Polym. Sci., Part A* **1994**, *32*, 3061−3067.
(6) Meyer, G. W.; Glass, T. E.; Grubbs, H. J.; McGrath, J. E. *Polym. Prepr.* **1994**, *35*, 549−550.
(7) Hergenrother, P. M.; Smith, J. G., Jr. *Polymer* **1994**, *35*, 4857 and references therein.
(8) Smith, J. G., Jr.; Hergenrother, P. M. *Polym. Prepr.* **1994**, *35*, 353−354.
(9) Jensen, B. J.; Bryant, R. G.; Wilkinson, S. P. *Polym. Prepr.* **1994**, *35*, 539−540.
(10) Havens, S. J.; Bryant, R. G.; Jensen, B. J.; Hergenrother, P. M. *Polym. Prepr.* **1994**, *35*, 553−554.
(11) Hinkley, J. A. *J. Adv. Mater.* **1994**, *27*, 55−59.
(12) Takekoshi, T.; Terry, J. M. *Polymer* **1994**, *35*, 4874−4880.
(13) Johnston, J. A.; Li, F. M.; Harris, F. W.; Takekoshi, T. *Polymer* **1994**, *35*, 4865−4873.
(14) Bryant, R. G.; Jensen, B. J.; Hergenrother, P. M. *Polym. Prepr.* **1993**, *34*, 566−567.
(15) Meyer, G. W.; Jayaraman, S.; McGrath, J. E. *Polym. Prepr.* **1993**, *34*, 540−541.
(16) Bryant, R. G.; Jensen, B. J.; Hergenrother, P. M. *Polym. Prepr.* **1992**, *33*, 910−911.
(17) For polycyclic end caps, see: Sutter, J. K.; Waters, J. F.; Schuerman, M. A. *Polym. Prepr.* **1992**, *33*, 366−367. Meader, M. A. B. *J. Polym. Sci., Part A* **1988**, *26*, 2907−2916. Scola, D. A. *J. Polym. Sci., Part A* **1993**, *31*, 2271−2286.
(18) For thermal curing acetylene-terminated resins, see: Sastri, S. B.; Keller, T. M.; Jones, K. M.; Armistead, J. P. *Macromolecules* **1993**, *26*, 6171−6174. Swanson, S. A.; Fleming, W. W.; Hofer, D. C. *Macromolecules* **1992**, *25*, 582−588. Lucotte, G.; Cormier, L.; Delfort, B. *J. Polym. Sci., Part A* **1991**, *29*, 897−903. Sefcik, M. D.; Stejskal, E. O.; McKay, R. A.; Schaefer, J. *Macromolecules* **1979**, *12*, 423−425.
(19) Neenan, T. X.; Whitesides, G. M. *J. Org. Chem.* **1988**, *53*, 2489−2496.
(20) Obata, Y.; Okuyama, K.; Kurihara, S.; Kitano, Y.; Jinda, T. *Macromolecules* **1995**, *28*, 1547.
(21) Dromzée, Y.; Kossanyi, J.; Wintgens, V.; Valat, P.; Biczók, Demeter, A.; Bérces, T. *Z. Kristallogr.* **1995**, *210*, 760.
(22) Schollmeyer, D.; Fischer, G.; Pindur, U. *Acta Crystallogr.* **1996**, *C52*, 1277.
(23) Hale, A.; Macosko, C. W.; Bair, H. E. *Macromolecules* **1991**, *24*, 2610−2621.
(24) Pascault, J. P.; Williams, R. J. J. *J. Polym. Sci., Part B* **1990**, *28*, 25.
(25) Couchman, P. R. *Macromolecules* **1987**, *20*, 1712−1717.
(26) DiBenedetto, A. T. *J. Polym. Sci., Part B* **1987**, *25*, 1949−1969.
(27) *teXsan for Windows, Version 1.05*; Molecular Structure Corp.: The Woodlands, TX, 1997−1999.
(28) Sheldrick, G. M. *SHELX 97: Program for the Refinement of Crystal Structures*; University of Göttingen: Göttingen, Germany, 1997.

MA000916Q